A study on Residual Drift and Concrete Strains in Unbonded Post-Tensioned Precast Rocking Walls

Sumedh Sharma[1], Sriram Aaleti[2]

[1] PhD Candidate, 2024 SERC building, Dept. of Civil, Const. & Env. Engineering, University of Alabama, Tuscaloosa, AL, USA 35487. Email: ssharma11@crimson.ua.edu;

[2] Assistant Professor, 2037 C SERC building, Dept. of Civil, Const. & Env. Engineering, University of Alabama, Tuscaloosa, AL, USA 35487. Email: saaleti@eng.ua.edu;

ABSTRACT

Modern seismic resistant design has been focusing on development of cost effective structural systems which experience minimal damage during an earthquake. Unbonded post-tensioned precast concrete walls provide a suitable solution due to their self-centering behavior and their ability to undergo large nonlinear deformation with minimal damage. Several experimental and analytical investigation focusing on lateral load resisting behavior of unbonded post-tensioned precast walls has been carried out in the past two decades. These investigations have primarily focused on lateral load resistance, self-centering capacity, energy dissipation and extent of damage in confined concrete region of the wall system. Past experimental results have shown that self-centering capacity of the wall system decreases at higher lateral drifts. Particularly, rocking walls with higher energy dissipation capacity, sustain considerable residual displacement. This residual displacement in the wall system may affect the ability of the entire structure to re-center. Though increasing initial prestressing force helps in reducing residual drift, it also subjects concrete to increased axial compressive stress which may lead to premature strength degradation of confined concrete in rocking corners. Accurate prediction of expected concrete strains in confined regions during increasing drift cycle is critical in design of such wall systems. Simplified design procedures available in literature assume different values for plastic hinge length to estimate critical concrete strain values. The results from the experimental tests available in literature were analyzed, to understand the effects of energy dissipating elements on residual drift and to examine the accuracy of simplified design procedures in predicting critical concrete strain. Based on the findings, recommendations are made on design of energy dissipating elements and plastic hinge length for unbonded post-tensioned precast rocking walls.

Keywords: Rocking walls, residual drift, concrete strain, plastic hinge length

INTRODUCTION

With advancement in seismic resistant design, the stakeholders are increasingly interested in structural systems which can undergo minimal damage during an earthquake event, have short functional downtime and can allow immediate occupancy. Unbonded post-tensioned precast rocking walls can meet such expectations due to their re-centering property and ability to undergo large deformations with minimal damage. In 1990s, the concept of self-centering unbonded post-tensioned jointed wall system was experimentally investigated as part of the Precast Seismic Structural Systems (PRESSS) research program [1]. After that, during past two decades, several large-scale experimental and analytical studies have been conducted and reported in the literature, demonstrating superior self-centering ability and minimal damage behavior of precast rocking walls compared to conventional monolithic reinforced concrete walls [2-8].

In recent times, there is a significant push towards improving the resiliency and move towards developing resiliency based design methodologies. In the case of unbonded post-tensioned rocking walls, the extent of residual drift plays an important role in determining resilient response of the overall structure. Typically, at design level earthquake loading, the post-tensioning (PT) in the concrete walls is designed to remain elastic, thus providing restoring force to reduce residual drift. As the PT tendons are designed to remain elastic, these wall systems are generally supplemented with additional energy dissipating hysteretic elements to ensure satisfactory energy dissipation during seismic loading. The response of such energy dissipating self-centering system is typically idealized by a flag-shaped hysteresis loop which assumes zero residual drift. However, a review of experimental testing results from the literature has shown that the unbonded post-tensioned walls do not strictly follow idealized flag shaped response [9]. Existing design guidelines recommend limiting moment contribution due to energy dissipating elements to 40% of the probable flexural capacity of the wall system to eliminate or minimize the residual drifts [10-11].

Increasing the amount of initial axial post-tensioning tendon (PT) force helps in increasing restoring moment and reducing residual drift for a given lateral drift. However, increased PT force will lead to increased compressive force at the rocking corners of the wall and it may result in nonlinear concrete response due to development of large compressive strains. Significant nonlinear concrete response eventually will lead to increase in residual drift. Also, the rocking corners of the walls should be designed with adequate confinement reinforcement to prevent premature crushing of confined concrete. Thus, it is critical to accurately predict critical compressive strains in the confined concrete region at the rocking wall corners. However, quantifying the usable concrete strain in unbonded post-tensioned walls is difficult due to rapid change in curvature at the wall base [12]. Simplified design procedures developed in literature aid designers in estimating concrete strains by assuming uniform distribution of inelastic curvature up to a certain fictitious height, commonly referred to as equivalent plastic hinge length. The simplified design procedures use different formulas for predicting the equivalent plastic hinge length [2] [13-15]. As shown later in this paper, the accuracy of plastic hinge length significantly affects the prediction of critical compressive strain in concrete.

A set of experimental results from the literature were analyzed to further understand the influence of energy dissipating elements on residual drift and examine the accuracy of equivalent plastic hinge lengths recommended in literature. For this paper, experimental test specimens having adequate experimental data for the required analysis, which are readily available were used in this study. Majority of the selected wall specimens were subjected to lateral load via actuators [2-4] [6] [8]; while one of them were subjected to shake table testing [7].

ANALYSIS ON RESIDUAL DRIFT

Recent experimental tests on unbonded post-tensioned precast walls consisting of two type of energy dissipating mechanisms, including Precast Wall with End Columns (PreWEC) walls with energy dissipating mild steel O-connectors at wall column interface [3] [6-8], and *hybrid* walls with energy dissipating reinforcement at wall foundation interface [2] [4-5] were examined in this study. Experimental data from a total of nine rocking wall specimens (6-PreWEC system and 3-hybrid walls) were analyzed to investigate the impact of initial PT force on residual drift and concrete strains.

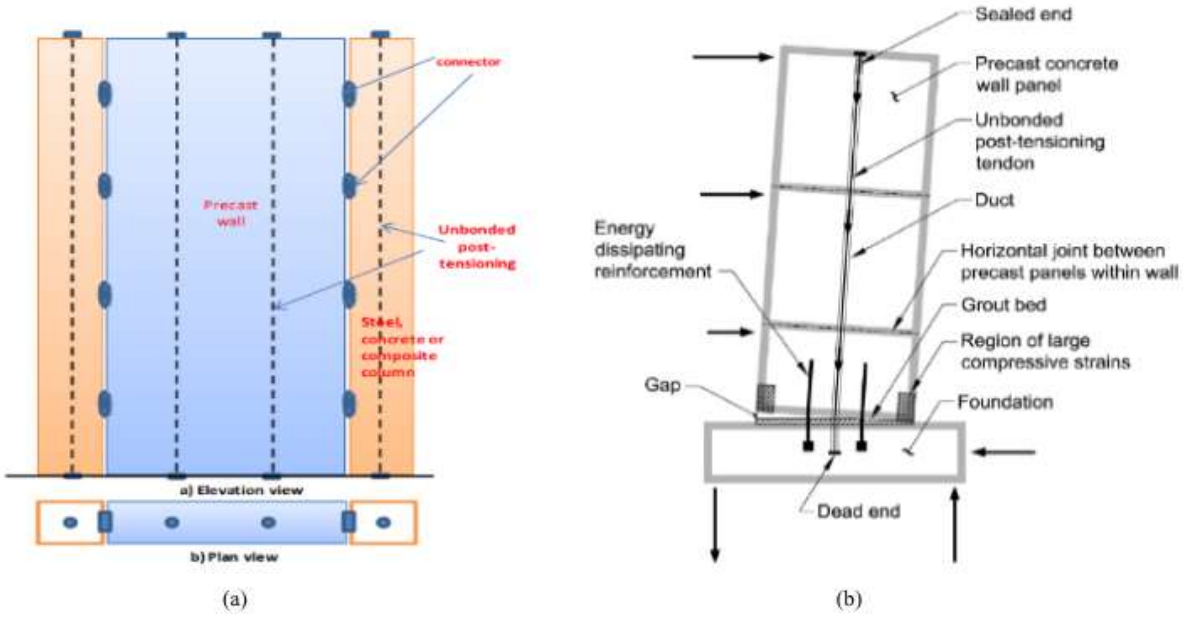

Figure 1 Schematic representation of (a) the PreWEC system [3] (b) hybrid wall system [16]

As seen in Figure 1a. PreWEC system consists of a post-tensioned precast wall connected to two, post-tensioned end columns using energy dissipating elements (O-connectors) along the vertical joint between the wall and column. The unbonded post-tensioning in all the elements are designed to remain elastic up to design drift. The walls and columns are designed to undergo rocking and uplift along the wall-to-foundation, column-to-foundation interface during lateral loading. Due to the uplift at wall and column base, a relative vertical displacement occurs along the vertical joint between the wall and columns. The connectors undergo vertical displacement and experience yielding during lateral loading and provide energy dissipation. The connectors are designed such that, they experience yielding before design drift level and do not rupture before 150% of the design drift level is achieved [16]. Upon removal of lateral load, the post-tensioning force in the elements causes the wall to re-center, forcing the connectors to come back to zero displacement. Due to the yielding, the connectors will experience residual forces at the zero displacement. These residual forces in O-connectors at different ends act on opposite direction to create an

overturning moment. ACI ITG 5.2 design provisions recommend strength of coupling devices should be small enough that effective prestress in the wall ensure that the residual drift for the coupled walls is zero when earthquake motions cease [16].

Table 1 shows extracted experimental data from six PreWEC system tests in the literature. The measured base shear, axial force including PT forces, self-weight of the specimens and externally applied axial force and relative vertical displacement of O-connectors were extracted at different lateral drift levels. The axial force (AF_o) presented in the table is the axial force recorded at the zero lateral force position, while unloading from respective peak drift level. With these data and experimentally measured force-displacement response of O-connectors, the moment capacity of the wall system at each drift level ($M_{wallsys}$) and the moment contribution due to energy dissipating connectors at that drift level (M_{ED}) were calculated. The overturning moment due to residual forces in the connectors at the zero lateral force level during unloading is denoted by M_{oED}. The decompression moment (M_{dec}) is the moment required to initiate the gap opening at the wall base and corresponds to zero tensile stress condition in the extreme concrete wall fiber. M_{dec}, M_{ED} and M_{oED} are calculated using formulas developed by Aaleti and Sritharan [15].

At higher drift level, the overturning moment due to O-connectors at zero lateral force position during unloading increases due to increase in residual forces in the O-connectors. On the contrary, the decompression moment decreases at higher drift due to subsequent loss in PT forces, which results in increase of (M_{oED}/M_{dec}) ratio at higher drift level. Once the overturning moment is greater than decompression moment, it results in residual gap opening at the base of the wall even when lateral force is absent. The variation of measured static residual drift (RD_{static}) with the ratio of (M_{oED}/M_{dec}) is shown in Figure 2a. Generally, when the overturning moment is greater than 1.5 times the decompression moment, a residual lateral drift greater than 0.15% is registered. However, in wall systems where concrete strains are significantly higher (i.e., PreWEC-1), residual drift is accumulated even before the (M_{oED}/M_{dec}) ratio is greater than 1. Figure 2a shows a nearly linear trend between (M_{oED}/M_{dec}) ratio and static residual drift. Thus, it is evident that residual forces present in the O-connectors contribute to residual drift. To negate such effects, it is necessary to design a wall system such that $M_{oED}/M_{dec} < 1$ and lower concrete strains in the rocking corners. Figure 2b shows the variation of static residual drift (RD_{static}) with the ratio of (M_{ED}/M_{wall}). The residual drift values keep increasing even though (M_{ED}/M_{wall}) value is similar and no significant trend can be observed. Thus, the (M_{ED}/M_{wall}) ratio is unable to capture the residual drift experienced by the wall system accurately. Therefore, the traditional design recommendation of limiting flexural contribution from energy dissipating members to 40% may not be adequate to ensure self-centering in PreWEC wall system. Also, this ratio may not be appropriate as a check to control the residual drifts in design guidelines of these systems.

Table 1. Analysis of residual drift of PreWEC system

Researcher	Specimen	Drift (%)	Base Shear (kN)	AF_o (kN)	$M_{wallsys}$ (kN-m)	M_{ED} (kN-m)	M_{oED} (kN-m)	M_{dec} (kN-m)	$\%M_{ED}$	RD_{static} (%)
Aaleti (2009) [3]	PreWEC-1	1	465.5	2058.6	2838.7	591.4	458.9	627.3	0.21	0.06
		1.5	486.8	2035.4	2967.7	605.2	564.6	620.3	0.20	0.18
		2	495.7	2012.7	3021.7	626.6	612.6	613.3	0.21	0.30
		2.5	501.5	1988.7	3057.0	647.9	636.2	606.0	0.21	0.44
Twigden et al. (2017) [8]	PreWEC-A2	1	79.2	333.8	238.1	65.2	54.3	44.5	0.27	0.11
		1.5	85.0	331.5	254.8	69.9	61.1	44.2	0.27	0.16
		2	88.1	329.3	264.7	72.3	65.3	43.9	0.27	0.24
		2.5	98.8	323.1	295.6	75.5	67.1	43.1	0.26	0.28
	PreWEC-B	1	94.3	332.0	282.5	76.0	76.0	44.3	0.34	0.18
		1.5	101.5	321.7	304.3	87.3	87.3	42.9	0.34	0.30
		2	106.8	312.8	319.9	96.1	96.1	41.7	0.34	0.46
		2.5	110.4	302.2	331.5	101.5	101.5	40.3	0.34	0.56
Nazari (2016) [7]	PreWEC-2	1	142.0	441.0	605.4	216.6	210.7	111.7	0.36	0.12
		1.5	153.1	441.0	652.7	233.9	222.8	111.6	0.36	0.16
		2	168.7	440.6	719.7	234.7	232.0	111.6	0.33	0.20
		2.5	171.3	439.7	730.1	244.7	238.8	111.3	0.34	0.32
	PreWEC-s2	1	164.2	526.0	699.8	298.2	208.5	167.4	0.43	0.34
		1.5	211.8	524.7	904.0	329.8	272.2	167.0	0.36	0.53
		2	223.8	523.8	955.1	337.9	315.2	166.6	0.35	0.72
		2.5	226.5	522.9	966.7	355.8	326.1	166.4	0.37	1.02
Liu (2016) [6]	PFS-2	1	237.2	817.5	1322.8	227.4	242.1	235.2	0.17	0.03
		1.5	250.1	811.7	1394.7	235.7	255.9	233.6	0.17	0.07
		2	259.0	794.3	1442.3	244.4	275.0	228.6	0.17	0.08

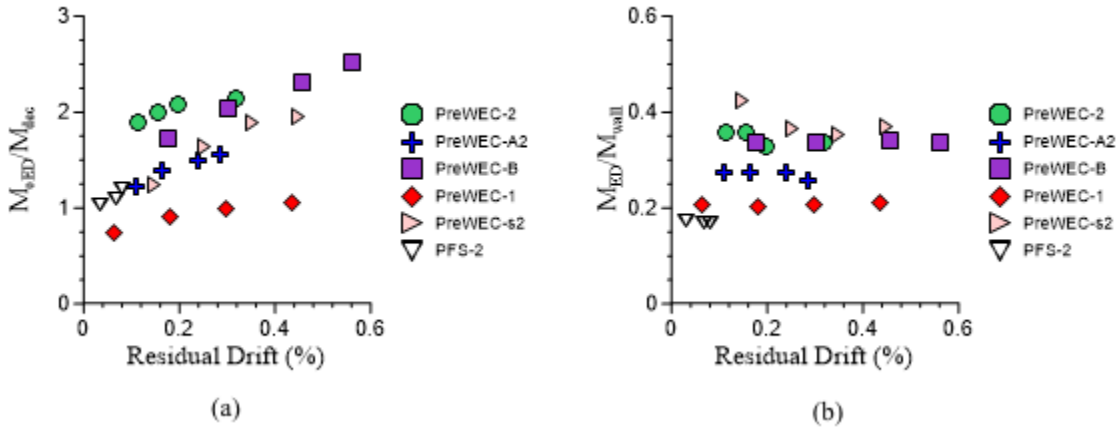

Figure 2. Experimental results of PreWEC wall systems (a) M_{oED}/M_{dec} vs residual Drift (b) M_{ED}/M_{wall} vs residual drift

Following the simplified design guidelines for a single wall PreWEC system [15]; with wall width of 'l_w', and 'npt' no. of tendons the decompression moment after design drift level loading is given by:

$$M_{dec} = \frac{1}{6} * l_w * \left[P_D + \sum_{i=1}^{npt} P_r\right] \quad (1)$$

where, P_r = PT forces in wall system at zero lateral force, while unloading from a design drift, P_D= externally applied additional axial force on the wall system including self-weight.

The overturning moment due to residual forces in O-connector about the centroid of the wall is given by:

$$M_{oED} = l_w * F_r * nconn \quad (2)$$

where, F_r = residual force in O-connectors at design drift which can conservatively be taken as rupture strength of the material, $nconn$ = no. of connectors per vertical joint.

From (1) and (2), for M_{oED}/M_{dec} <1

$$\frac{M_{oED}}{M_{dec}} = \frac{l_w * F_r * nconn}{\frac{1}{6} * l_w * \left[P_D + \sum_{i=1}^{npt} P_r\right]} \leq 1 \quad (3)$$

Rearranging equation (3),

$$F_r * nconn \leq \frac{1}{6} * \left[P_D + \sum_{i=1}^{npt} P_r\right] \quad (4)$$

Therefore, to ensure adequate self-centering of PreWEC wall system, the connectors should be designed such that total residual forces acting on connectors per joint should be less than 1/6th of the available restoring force at the re-centered position of the wall.

In *hybrid* walls, the energy dissipating elements are the longitudinal mild-steel rebar passing across the wall-foundation interface. The mild steel bars are ideally designed to yield in compression and tension during application of lateral loading. Generally, these energy dissipating rebars (ED bars) are placed close to center of the wall and debonded over a certain height to reduce localized tensile stresses and premature fracture at lower drifts. At lateral drift levels more than 0.5%, the neutral axis depth (i.e., contact length at the wall base) gets shorter and moves further away from the center of the wall. In such cases, all ED bars are on tension side at peak drift and undergo tensile deformation. Under removal of lateral load, the residual forces in the ED bars act in same direction. Thus, they do not create significant overturning moment as in the case of O-connectors in PreWEC system. However, upon unloading the restoring axial force from PT force and externally applied axial load should be sufficient to yield the ED bars back in compression so that the gap at the base of the wall is closed [4]. Table 2 shows extracted experimental data from three hybrid wall systems in the literature. The moment contribution due to PT force and externally

applied axial load including self-weight is denoted by M_{PT}. M_{PT} is calculated by taking moment of PT force in each tendon and the externally applied axial force including self-weight about the compression resultant assumed to be at half of the neutral axis depth. The moment contribution due to ED bars (M_{ED}) is taken as difference between $M_{wallsys}$ and M_{PT}. At each peak drift level, the restoring PT force and axial load is calculated and tabulated under F_{res}. F_{reqd} is the theoretical restoring force required to yield back in compression the ED bars which are at ultimate tensile stress at peak drift level. F_{reqd} is calculated as the product of sum of yield stress and ultimate stress of ED bars (i.e f_y+f_u) with the area of ED bars.

Walls HW1 and HW3 have more than 90% of the theoretical restoring force required to close the gap at the base of the wall. Wall HW5 has roughly 60% of the theoretical restoring force required to close the gap. This difference is one of the causes for the residual drift in wall HW5 to be nearly three times of wall HW1 and HW3. As the restoring force in HW5 is not enough to yield the ED bars back in compression, a gap is formed throughout the base of the wall. This residual uplift eventually effects the walls ability to recenter and causes higher residual drift. In case of *hybrid* walls, the traditional design guideline of limiting moment contribution due to ED bars to 40% of probable flexural capacity of the wall systems seems reasonable. In case of wall HW5, the contribution due to ED bars is close to 50% resulting in higher residual drift.

Table 2. Analysis of residual drift of Hybrid Wall system

Researcher	Specimen	Drift (%)	Base Shear (kN)	$M_{wallsys}$ (kN-m)	M_{PT} (kN-m)	M_{ED} (kN-m)	$\%M_{ED}$	F_{res} (kN)	F_{reqd} (kN)	RD_{static} (%)
Smith et al. (2013)[4]	HW1	1	533.1	1949.5	1174.5	775.0	0.40	1127.2	1199.3	0.05
		1.5	514.9	1881.9	1127.3	754.5	0.40	1168.1		0.07
		1.9	418.7	1531.5	1023.2	508.3	0.33	1144.5		0.12
	HW3	1	541.6	1980.0	1214.9	765.0	0.39	1142.3	1259.4	0.04
		1.5	549.1	2008.6	1258.4	750.2	0.37	1186.4		0.07
		2	511.8	1870.8	1199.2	671.6	0.36	1207.3		0.13
		2.5	439.2	1606.2	1129.1	477.1	0.30	1173.0		0.14
	HW5	1	593.6	2170.2	820.3	1349.9	0.62	1080.0	1794.7	0.12
		1.5	610.1	2231.5	1054.5	1177.0	0.53	1134.3		0.28
		2	620.8	2269.6	1155.2	1114.4	0.49	1167.2		0.33
		2.3	627.0	2292.2	1201.6	1090.7	0.48	1199.3		0.35

To prevent excessive residual uplift and subsequent residual drift in *hybrid* walls the restoring force at peak design drift should be sufficient to yield the ED bars back in compression. For a wall system with ED bars of yield stress(f_y) and ultimate tensile stress (f_u) and ED bar area of A_{ED}, F_{reqd}can be written as:

$$F_{reqd} = A_{ED} * (f_y + f_u) \tag{5}$$

The restoring force F_{res} at peak drift is summation of axial PT force at peak drift P_P and externally applied axial force on the wall system including self-weight P_D.To ensure adequate self-centering, at design drift level $F_{reqd}/F_{res} \leq 1$.

$$\frac{F_{reqd}}{F_{res}} = \frac{A_{ED}*(f_y+f_u)}{P_P+P_D} \leq 1 \tag{6}$$

Rearranging equation (6),

$$A_{ED} \leq \frac{P_P+P_D}{(f_y+f_u)} \tag{7}$$

Equation (7) provides the maximum limit for area of ED bars to ensure adequate self-centering in case of *hybrid* walls. Some experimental [7] [17] and analytical study [9] have shown that final residual drift of rocking walls at the end of earthquake shaking is lower compared to peak residual drift during shaking. Incorporating such reductions increases limits on numbers of O-connectors and area of ED bars.

ANALYSIS ON CONCRETE STRAIN

Several simplified design procedures available in literature predict concrete strain at a given base rotation (ε_θ) by equating the curvature $(\emptyset_\theta)$ at the base of the wall with corresponding neutral axis depth (c_θ).

$$\varepsilon_\theta = \emptyset_\theta * c_\theta \tag{8}$$

The curvature is estimated by assuming the displacement of the wall is due to contributions from concentrated plastic rotation at the base, flexural deformation, shear deformation and slip at the base. The shear deformation and slip of the wall is generally

neglected for simplicity, as their contribution towards total lateral deformation is small. In unbonded rocking walls, the wall specimen doesn't experience shear damage unlike the traditional reinforced concrete wall. The plastic hinge region at the base is assumed to have uniform inelastic curvature up to a certain height referred to as equivalent plastic hinge length (L_p). Several equations available in literature for calculating the equivalent the plastic hinge length in unbonded post-tensioned rocking walls are presented in Table 3 below.

Table 3. Equations for plastic hinge length

Researchers	**Plastic Hinge Length (L_p)**	**Description**
Rahman & Restrepo (2000)[13]	c	c = neutral axis depth
Perez (2004)[2]	t_w'', if $t_w''<2a''$ $2a''$, if $2a''<t_w''$	t_w''= wall thickness measured between confinement reinf. a''= equivalent confined concrete stress block measured from confinement reinf.
Kurama (2005)[14]	0.2 L_w	L_w=length of wall
Aaleti & Sritharan (2009)[15]	0.06 h_w	h_w= height corresponding to lateral load location

A set of experimental data was analyzed to check the accuracy of plastic hinge length proposed by different researchers. The total curvature at the base of the wall ($\emptyset_t$) at given drift level was calculated from the extracted neutral axis depth (c_θ) and concrete strain value (ε_θ) recorded by strain gauge located at distance ($\mathrm{d_{sg}}$) from the edge of the wall.

$$\emptyset_t = \frac{\varepsilon_\theta}{(c_\theta - \mathrm{d_{sg}})} \tag{9}$$

Subtracting elastic curvature $\emptyset_e$ from total curvature $\emptyset_t$ gives the plastic curvature $\emptyset_p$ at the given drift level.

$$\emptyset_p = \emptyset_t - \emptyset_e \tag{10}$$

The elastic curvature is given by:

$$\emptyset_e = \frac{M}{E_c * I_c} \tag{11}$$

Where, M = moment at the base of the wall (kip-in), E_c = modulus of elasticity of concrete (ksi), I_c = moment of inertia of concrete section (ksi).

Once the plastic curvature is known, the plastic hinge length compatible with experimental results is calculated as:

$$L_p = \frac{\Delta_t - \Delta_e}{\emptyset_p * h_w} \tag{12}$$

Where, Δ_t = total displacement at the top of the wall, Δ_e = displacement at the top of the wall due to elastic flexural deformation, h_w = height of the wall

Table 4 shows the comparison of experimentally obtained equivalent plastic hinge length at 2% lateral drift with that calculated from equations presented in Table 3.From the table it is evident that the analytical equations found in simplified design procedures are not consistent in predicting plastic hinge length. The predictions from analytical equations are relatively accurate in certain walls (TW1, TW2, PreWEC); but are significantly different in case of other walls. The analytical equations given by Kurama and Aaleti & Sritharan are only dependent on geometry of the wall system. The analytical equations by Rahman & Restrepo and Perez indirectly account for axial compressive force by relating plastic hinge length with neutral axis depth. However, they do not consistently predict plastic hinge length over different wall system.

Therefore, concrete strain and plastic hinge length were studied relative to axial force ratio. The axial force ratio (AFR) is calculated as $AFR = (P + N)/(A_g * f_c')$, where P represents the initial post-tensioning force, N is the externally applied axial force, $\mathrm{A_g}$ is the gross cross section area of the wall and f_c' is the compressive strength of concrete. The plastic hinge length was normalized with respect to one of the geometric property (height of the wall) to study adequacy of conventional plastic hinge equation. The comparisons in Table 4 are made at drift level of 2%. In the wall tests, the concrete strain measurements were

taken within 1.5 to 4 in. from the rocking edge of the wall. Figure 3a shows the expected trend of increasing concrete strain with increasing axial force ratio. Figure 3b shows that a single ratio of (L_p/h_w) is insufficient to accurately predict concrete strain for all the experimental tests. Combining inputs from Figure 3a and Figure 3b, it can be inferred that L_p/h_w is lower for wall systems with higher AFR when compared to wall systems with lower AFR. Figure 3(c) shows that generally L_p/h_w ratio is higher (0.2-0.3) for AFR lower than 0.1 and lower (0.05-0.1) for AFR greater than 0.1. A linear fit of the plot in Figure 3c equated plastic hinge length with AFR as $\left[\frac{L_p}{h_w} = 0.22 - 0.64 * (AFR)\right]$. More experimental data is required to improve on the above plastic hinge length equation. However, it is enough to conclude that the analytical equations available for prediction of concrete strain in simplified design procedures are inaccurate due to wrong assumption of plastic hinge length. Additionally, recent tests on walls having AFR lower than 0.1 has shown that experimentally recorded strain values were lower than analytically predicted ones [5] [16]. This is consistent, with the finding from Figure 3c as the analytical equations generally under predict plastic hinge lengths for walls with AFR lower than 0.1 which leads to over prediction of concrete strains.

Table 4. Comparison of experimental and analytically predicted plastic hinge lengths

Researcher	Specimen	L_p (exp) (mm.)	L_p (Rahman & Restrepo) (mm.)	L_p (Perez) (mm.)	L_p (Kurama) (mm.)	L_p (Aaleti & Sritharan) (mm.)
Perez et al.(2004)[2]	TW1	447	518	152	508	434
	TW2	671	493	152	508	434
	TW3	1405	589	152	508	434
	TW4	759	432	152	508	434
	TW5	1120	373	152	508	434
Aaleti (2009)[3]	PreWEC	305	277	152	366	366
Liu (2016)[6]	PFS-2	1516	213	152	345	335
Twigden et al.(2017)[8]	SRW-A	312	71	119	198	188
	SRW-B	889	119	124	160	180
	PreWEC-B	544	109	124	160	180

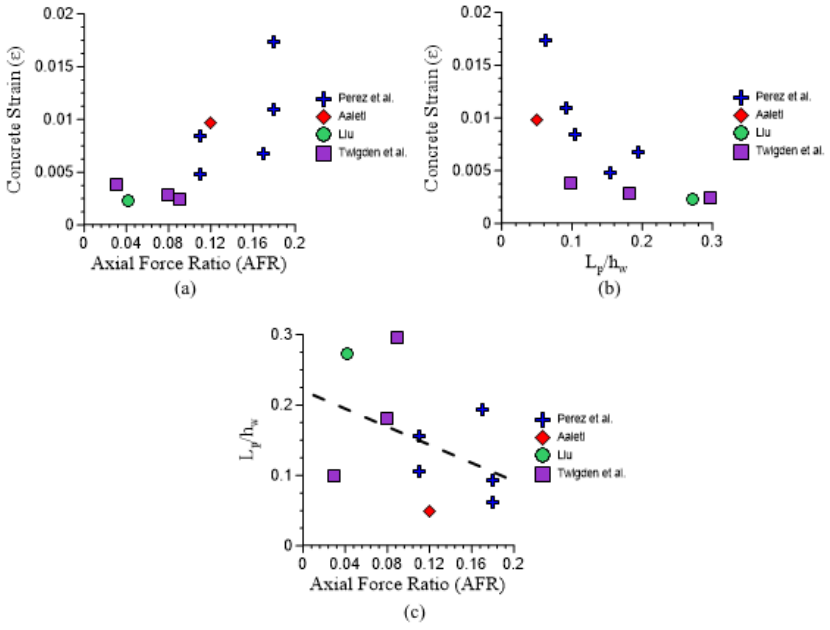

Figure 3. *Experimental Result of Unbonded Post-Tensioned Walls at Drift Level of 2% (a) Concrete Strain vs Axial Force Ratio (AFR) (b) Concrete Strain vs L_p/h_w (c) L_p/h_w vs Axial Force Ratio (AFR)*

CONCLUSIONS

The analysis of experimental data shows residual drift of an unbonded post-tensioned precast wall to be influenced by energy dissipating elements. In PreWEC wall systems, the residual forces in O-connectors provide overturning moment which if higher

than decompressing moment induces residual drift. To prevent it, the connectors should be designed such that total residual forces acting on connectors per joint should be less than $1/6^{th}$ of the available restoring force at the re-centered wall position. The traditional approach of limiting moment contribution due to energy dissipating element to 40% was found to be insufficient to limit residual drift in PreWEC systems. In *hybrid* walls, the restoring force at design drift should be enough to yield the ED bars back in compression. Otherwise, the gap at the base of the wall remains unclosed and contributes to higher residual drift. Thus, energy dissipating elements should be carefully designed according to wall systems to ensure adequate self-centering of the wall system. The analysis of experimental data with respect to concrete strains showed plastic hinge length to be dependent on Axial Force Ratio (AFR). The equations used for prediction of plastic hinge length in existing simplified design procedures were found to be inaccurate. A new equation for calculating plastic hinge length was developed: $\left[\frac{L_p}{h_w} = 0.22 - 0.64 * (AFR)\right]$. There is need for more experimental data points at different AFR to improve upon above relationship for plastic hinge length.

ACKNOWLEDGMENTS

The study reported in this paper is supported by the National Science Foundation through the Engineering for Natural Hazards (ENH) program (grant number 1662963). Any opinions, findings, and conclusions expressed in this paper are those of the authors, and do not necessarily represent those of the sponsor.

REFERENCES

[1] Priestley, M. J. N., Sritharan, S., Conley, J.R., and Pampanin, S. (1999). "Preliminary results and conclusion from the PRESS five- story precast concrete test building". *PCI Journal*, 44(6), 42-67.

[2] Perez, F. J., Pessiki, S., and Sause, R. (2004). *Experimental and analytical lateral load response of unbonded post-tensioned precast concrete walls.* ATLSS report no. 04-11, ATLSS, Lehigh Univeristy, Bethlehem, PA.

[3] Aaleti, S. (2009). *Behavior of rectangular concrete walls subjected to simulated seismic loading, Phd Thesis.* Graduate Theses and Dissertations. 11047, Iowa State University, Ames, Iowa.

[4] Smith, B. J., Kurama, Y.C., and McGinnis, M. J. (2012). *Hybrid precast wall systems for seismic regions.* Report no. NDSE-2012-01, Structural Eng. Research Report, Dept. of Civil Eng. and Geological Sciences, Univ. of Notre Dame, Notre Dame, Indiana

[5] Belleri, A., Schoettler, M. J., Restrepo, J. I., and Fleischman, R. B. (2014). "Dynamic behavior of rocking and hybrid cantilever walls in a precast concrete building". *ACI Structural Journal*, 111(3), 661-671.

[6] Liu, Q. (2016). *Study on interaction between rocking-wall system and surrounding structure, Phd Thesis.* Retrieved from University of Minnesota Digital Conservancy, http://hdl.handle.net/11299/185155.

[7] Nazari, M. (2016). *Seismic performance of unbonded post-tensioned precast wall systems subjected to shake table testing,Phd Thesis.* Graduate Theses and Dissertations. 15778., Iowa State University,Ames,Iowa.

[8] Twigden, K.M., Sritharan, S., and Henry, R. (2017). "Cyclic testing of unbonded post-tensioned concrete wall systems with and without supplemental damping." *Engineering Structures*,140, 406-420.

[9] Henry, R. S., Sritharan, S., & Ingham, J. M. (2016). "Residual drift analyses of realistic self-centering concrete wall systems". *Earthquake and Structures*, 10(2),409-428.

[10] ACI Innovation Task Group 5 (2007). *Acceptance criteria for special unbonded post-tensioned precast structural walls based on validation testing (ITG 5.1-07).* American Concrete Insititute, Farmington Hills, Masachusetts.

[11] Pampanin, S., Mariott, D., and Palermo, A. (2010). *PRESS design handbook.* New Zealand Concrete Society, Auckland.

[12] Henry, R., Brooke, N.J., Sritharan, S., and Ingham, J. (2012). "Defining concrete compressive strain in unbonded post-tensioned walls". *ACI Structural Journal,* 109(1), 101-111.

[13] Rahman, A.M., and Restrepo, J.I. (2000). *Earthquake resistant precast concrete buildings: seismic performance of cantilever walls prestressed using unbonded tendons.*Research Report no. 2000-5,Dept. of Civil Eng., Univ. of Canterbury, Canterbury

[14] Kurama, Y. C.(2005). "Seismic design of partially post-tensioned precast concrete walls". *PCI Journal*, 50(4),100-125.

[15] Aaleti, S., and Sritharan, S. (2009). "A simplified analysis method for characterizing unbonded post-tensioned precast wall systems". *Engineering Structures*, 31(2009), 2966-2975.

[16] ACI Innovation Task Group 5 (2009). *Requirements for design of a special unbonded post-tensioned precast shear wall satisfying ACI ITG-5.1 (ITG 5.2-09),*American Concrete Insititute, Farmington Hills, Masachusetts.

[17] Twigden, K. M. (2016). *Dynamic response of unbonded post-tensioned concrete walls for seismic resilient structures,Phd Thesis.* University of Auckland, Auckland.